Hindawi Publishing Corporation
International Journal of Chemical Engineering
Volume 2014, Article ID 256840, 7 pages
http://dx.doi.org/10.1155/2014/256840

Research Article

Numerical Simulation and Analysis of CO_2 Removal in a Polypropylene Hollow Fiber Membrane Contactor

Zhien Zhang, Yunfei Yan, Li Zhang, and Shunxiang Ju

Key Laboratory of Low-Grade Energy Utilization Technologies and Systems, Chongqing University, Chongqing 400044, China

Correspondence should be addressed to Yunfei Yan; yunfeiyan@cqu.edu.cn

Received 19 July 2013; Revised 1 December 2013; Accepted 20 December 2013; Published 30 January 2014

Academic Editor: Mahesh T. Dhotre

This present study shows a comprehensive 2D numerical model for removal of CO_2 in a polypropylene (PP) hollow fiber membrane contactor (HFMC) using the computational fluid dynamics (CFD) method. Monoethanolamine (MEA) solution was used as the liquid absorbent in a nonwetting mode. The simulation results represented that higher liquid velocity and concentration and lower gas velocity and concentration led to higher percent of CO_2 removal. The most proper parameters for CO_2 removal were less than 1 mol m^{-3} gas concentration and 0.2 m s^{-1} gas flow rate, and for MEA the values were above 8 mol m^{-3} concentration and approximately 1 m s^{-1} liquid velocity. Furthermore, the model was validated with the experiment results. Therefore, the modeling results provided references to the selection of absorbents and operation parameters in the experimental study and pilot-scale applications.

1. Introduction

In recent years, human-induced CO_2 severely results in global climate change [1]. Especially the combustion of fossil fuels produces a large number of gas emissions. So capturing CO_2 from flue gas in the postcombustion process will be an effective way to reduce CO_2 emissions. Nowadays several methods of CO_2 removal have been used like adsorption, chemical and physical absorption, and membrane separation. But conventional absorption methods have plenty of shortcomings such as flooding, foaming, channeling, air entrainment, and high capital and operational costs [2, 3]. In order to solve those problems, the membrane gas absorption which combines the merits of membrane separation and chemical absorption is gradually introduced by some researchers. In a hollow fiber membrane contactor, the absorbent always flows on one side while gas mixture flows in the other side. Meanwhile, a gas-liquid interface is formed at membrane pores, which are filled with gases. In the membrane absorption process, gas mixture initially diffuses through the gas-liquid interface, and then CO_2 reacts with the liquid. After that the rich liquid is sent into a gas-liquid separator or other membrane contactors. Ultimately the lean solution flows back to the membrane contactor for recycling. Compared with conventional absorption technologies, the gas membrane separation provides faster mass transfer rate, good operational flexibility, and bigger gas-liquid contacting area. Therefore, it runs well without entrainment, flooding, foaming, and so forth. And this technique is considered to be a promising large-scale application of CO_2 capture [4, 5].

Since Qi and Cussler [6] first investigated the hollow membrane contactor, a large number of scholars studied gas absorption in these devices in succession. Al-Marzouqi et al. [7] performed chemical absorption of CO_2 from CO_2/CH_4 gas mixture in a membrane contactor module using MEA and NaOH solutions. They developed a PVDF membrane contactor model on the conditions of complete and partial wetting. Meanwhile, they also used distilled water and MEA for absorbing CO_2 from gas mixture in nonwetting mode [8]. A similar system was performed by Ghadiri et al. [9]. Zhang et al. [10] investigated the CO_2 absorption from a CO_2/N_2 gaseous mixture in a hollow fiber membrane using alkanolamine solutions including DEA and water. The gas-liquid contacting process was assumed at different membrane wetting degrees. Additionally, a membrane model of CO_2 removal using potassium glycinate (PG) solution was built

up by Eslami et al. [11]. They investigated the effects of PG concentration, liquid velocity, and liquid temperature on CO_2 absorption performance in this work.

Some scholars experimented and simulated on the absorption of pure CO_2. Rajabzadeh et al. [12, 13] performed the capture of pure CO_2 using MEA solutions in polyvinylidene fluoride (PVDF) HFMCs and compared the difference between PVDF and polytetrafluoroethylene (PTFE). Rongwong et al. [14] studied the CO_2 removal using MEA solutions in membrane modules and made a comparison of theoretical results with experimental data. In the process of CO_2 membrane absorption, PG and 2-amino-2-methyl-1-propanol (AMP) were used as a blended solvent in nonwetting mode [15]. It is well known that MEA is a high-effective absorbent of absorbing CO_2, which attracts many scholars' interests [16, 17].

The aim of the current study is to develop and solve a comprehensive 2D model for CO_2-MEA system, which is based on the nonwetting mode in a HFMC. Assuming the axial and radial diffusion inside the tube side, membrane and the shell side are investigated in this model. The paper focuses on the effects of the gas concentration, gas velocity, liquid concentration, and liquid velocity. Yet still, there is no literature discussing the influence on gas concentration using a PP HFMC and comprehensive consideration of liquid and gas properties. And this is the first time to compare the experimental data with simulation results in such a CO_2-MEA system.

2. Model Development

In this work, a steady state 2D mathematical model was developed to describe the absorption process of pure CO_2 using aqueous MEA solutions. Figure 1 shows a schematic diagram of a HFMC material module used in the model development. In this case, the liquid absorbent flows into the tube side (at $z = 0$), while CO_2 flows in the shell side (at $z = L$) in a counter-current arrangement. Firstly, CO_2 diffuses from the gas phase to the liquid phase through the membrane pores. And then they react with the absorbents in the tube.

2.1. Tube Side Equations. The steady state continuity equation for the transport and reaction of one species in the tube side due to diffusion, reaction, and convection may be written as

$$D_{i\text{-tube}}\left[\frac{\partial^2 C_{i\text{-tube}}}{\partial r^2}+\frac{1}{r}\frac{\partial C_{i\text{-tube}}}{\partial r}+\frac{\partial^2 C_{i\text{-tube}}}{\partial z^2}\right] = V_{z\text{-tube}}\frac{\partial C_{i\text{-tube}}}{\partial z}-R_i, \tag{1}$$

in which i is CO_2 or absorbent. Meanwhile, $D_{i\text{-tube}}$, $C_{i\text{-tube}}$, R_i, and $V_{z\text{-tube}}$ denote the diffusion coefficient, the concentration, the reaction rate of species I, and the axial velocity inside the fiber tube, respectively. Especially when using a chemical sorbent like MEA, R_{CO_2} could be approximated by

$$R_{CO_2} = -k_r\left[CO_2\right]\left[\text{MEA}\right], \tag{2}$$

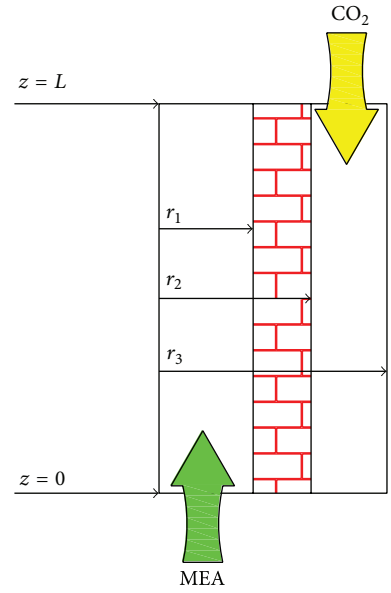

Figure 1: A schematic diagram of a hollow fiber membrane model.

where the reaction rate constant k_r under the conditions of 298 K and 1 atm can be estimated as follows [18]:

$$k_r = \frac{10^{(10.99-2152/T)}}{1000}. \tag{3}$$

The axial velocity distribution inside the tube is assumed to follow the Newtonian laminar flow [19]:

$$V_{z\text{-tube}} = 2\overline{V}_{\text{tube}}\left[1-\left(\frac{r}{r_1}\right)^2\right], \tag{4}$$

where $\overline{V}_{\text{tube}}$ and r_1 are the average gas velocity in the tube side and the inner tube radius, respectively.

Boundary conditions are given as

$$\begin{aligned} &\text{at } r = 0, \quad \frac{\partial C_{i\text{-tube}}}{\partial r} = 0 \quad (\text{symmetry}),\\ &\text{at } r = r_1, \quad C_{CO_2\text{-tube}} = m \times C_{CO_2\text{-membrane}},\\ &\frac{\partial C_{\text{absorbent-tube}}}{\partial r} = 0 \quad (\text{nonwetting mode}),\\ &\text{at } z = 0\ (\text{inlet}), \quad C_{\text{absorbent-tube}} = C_{\text{absorbent-tube, initial}},\\ &C_{CO_2\text{-tube}} = 0, \end{aligned} \tag{5}$$

where m, $C_{CO_2\text{-membrane}}$, and $C_{\text{absorbent-tube, initial}}$ denote the CO_2 solubility in the aqueous solution, the CO_2 concentration inside the membrane, and the absorbent concentration in the fiber tube, respectively.

2.2. Membrane Equations (Nonwetting Mode). In a nonwetting mode CO_2 only diffuses in the membrane. So the steady

state continuity equation for transport of CO_2 inside the membrane could be written as

$$D_{CO_2\text{-membrane}}\left[\frac{\partial^2 C_{CO_2\text{-membrane}}}{\partial r^2}+\frac{1}{r}\frac{\partial C_{CO_2\text{-membrane}}}{\partial r}+\frac{\partial^2 C_{CO_2\text{-membrane}}}{\partial z^2}\right]=0, \tag{6}$$

where $D_{CO_2\text{-membrane}}$ is the diffusion coefficient in the membrane.

Considering the influences of the porosity and tortuosity of the membrane on the absorption performance, $D_{CO_2\text{-membrane}}$ may be written as

$$D_{CO_2\text{-membrane}}=\frac{D_{CO_2\text{-shell}}\times\varepsilon}{\tau}, \tag{7}$$

where $D_{CO_2\text{-shell}}$, ε, and τ are the effective diffusion coefficient inside the shell, the membrane porosity, and the membrane tortuosity, respectively.

Boundary conditions are given as

$$\begin{aligned}&\text{at } r=r_1, \quad C_{CO_2\text{-membrane}}=\frac{C_{CO_2\text{-tube}}}{m},\\&\text{at } r=r_2, \quad C_{CO_2\text{-membrane}}=C_{CO_2\text{-shell}},\end{aligned} \tag{8}$$

where $C_{CO_2\text{-shell}}$ is the concentration of CO_2 in the shell side.

2.3. Shell Side Equations. The steady state continuity equation for CO_2 transport inside the shell where only CO_2 flows could be defined as

$$D_{CO_2\text{-shell}}\left[\frac{\partial^2 C_{CO_2\text{-shell}}}{\partial r^2}+\frac{1}{r}\frac{\partial C_{CO_2\text{-shell}}}{\partial r}+\frac{\partial^2 C_{CO_2\text{-shell}}}{\partial z^2}\right]=V_{z\text{-shell}}\frac{\partial C_{CO_2\text{-shell}}}{\partial z}. \tag{9}$$

According to Happel's free surface theory, the axial velocity $V_{z\text{-shell}}$ in the shell may be estimated as follows [20]:

$$V_{z\text{-shell}}=2\overline{V}_{\text{shell}}\left[1-\left(\frac{r_2}{r_3}\right)^2\right]\times\left[\frac{(r/r_3)^2-(r_2/r_3)^2+2\ln(r_2/r)}{(r_2/r_3)^4-4(r_2/r_3)^2+4\ln(r_2/r_3)+3}\right], \tag{10}$$

in which $\overline{V}_{\text{shell}}$ and r_2 are the gas average velocity inside the shell and the outer fiber radius, respectively. At the same time, the inner shell radius r_3 may be written as

$$r_3=r_2\sqrt{\frac{1}{1-\phi}}, \tag{11}$$

where ϕ represents the volume fraction of the void in the shell side and could be estimated by

$$1-\phi=\frac{nr_2^2}{R^2}, \tag{12}$$

Table 1: Dimensions and properties of the membrane contactor module.

Parameter	Value	Reference
Inner tube radius (mm)	0.15	Membrane manufacture
Outer tube radius (mm)	0.2	Membrane manufacture
Inner shell radius (mm)	0.3	Calculated
Module length (mm)	900	Membrane manufacture
Number of fibers	3000	Membrane manufacture
Membrane porosity/tortuosity	0.7/2	Membrane manufacture
$D_{CO_2\text{-tube}}$ ($m^2\ s^{-1}$)	1.51×10^{-9}	[23]
$D_{CO_2\text{-shell}}$ ($m^2\ s^{-1}$)	1.8×10^{-5}	[24]
$D_{CO_2\text{-membrane}}$ ($m^2\ s^{-1}$)	6.34×10^{-6}	Calculated
$D_{MEA\text{-tube}}$ ($m^2\ s^{-1}$)	7.55×10^{-10}	Calculated
$D_{MEA\text{-membrane}}$ ($m^2\ s^{-1}$)	2.64×10^{-10}	Calculated
m	0.8314	[23]
k_r ($m^3\ mol^{-1}\ s^{-1}$)	5.868	Calculated

where n and R denote the number of fibers and the inner module radius, respectively.

Boundary conditions are given as

$$\begin{aligned}&\text{at } r=r_2, \quad C_{CO_2\text{-shell}}=C_{CO_2\text{-membrane}},\\&\text{at } r=r_3, \quad \frac{\partial C_{CO_2\text{-shell}}}{\partial r}=0 \quad (\text{symmetry}),\\&\text{at } z=L, \quad C_{CO_2\text{-shell}}=C_0 \quad (\text{inlet}).\end{aligned} \tag{13}$$

3. Numerical Solution

To solve the above equations, the module dimensions and physical and chemical properties are provided in Table 1. The above dimensionless model equations associated with the tube, membrane, and shell sides with the appropriate boundary conditions and properties were solved using a COMSOL Multiphysics software, which uses the computational fluid dynamics (CFD) method for numerical solutions of model equations. For the finite element analysis, the solver of UMFPACK is applied owing to memory efficiency. And this method is combined with adaptive meshing and error control. This solver, an implicit time-stepping scheme, is well suited for solving stiff and nonstiff nonlinear boundary value problems.

4. Results and Discussion

4.1. Model Validation. In order to validate the developed model, Figure 2 shows a comparison between experimental data and modeling predictions at different values of the absorbent concentration. The membrane parameters used in the simulations are the same as those in experiments.

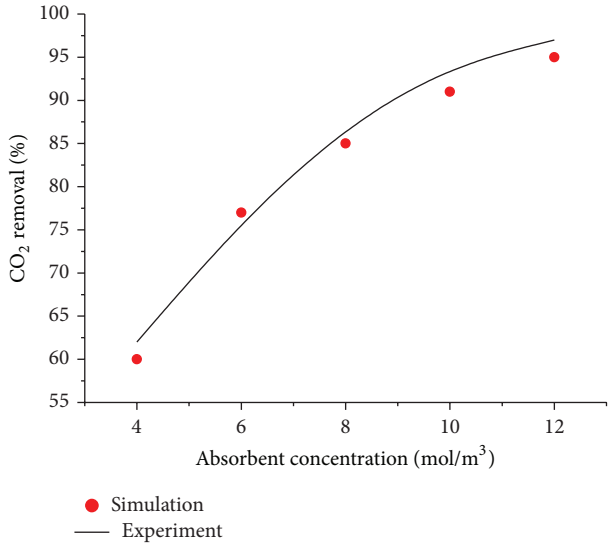

FIGURE 2: Comparison of simulation values with experiment results. $C_0 = 4\,\text{mol m}^{-3}$, $v_{CO_2} = 0.2\,\text{m s}^{-1}$, $v_{MEA} = 0.5\,\text{m s}^{-1}$.

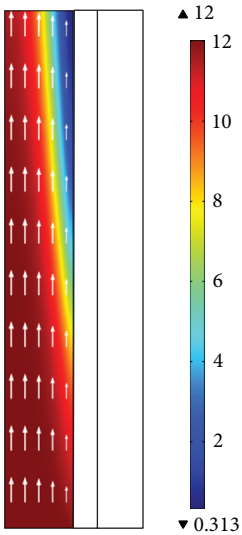

FIGURE 3: Flux vectors and concentration distribution of MEA in the model. $C_0 = 4\,\text{mol m}^{-3}$, $C_{MEA,0} = 12\,\text{mol m}^{-3}$, and $v_{MEA} = 0.5\,\text{m s}^{-1}$.

The hydrophobic PP hollow fiber membranes were purchased from Hangzhou Kaihong Membrane Technology Co., Ltd. The CO_2 cylinder was purchased from Chongqing Ruike Gas Co., Ltd. and the aqueous MEA solution was purchased from Chongqing Dongfanghuaba Co., Ltd. $4\,\text{mol m}^{-3}$ MEA was used as the absorbent in a PP HFMC. It is obvious that the CO_2 removal rate goes up with an increase of liquid absorbent concentration. Additionally, the absorption rates calculated by this model are in well agreement with experiment results.

4.2. Concentration Distribution and Flux Vectors. When using $12\,\text{mol m}^{-3}$ MEA aqueous solution as the solvent, the concentration distribution and flux vectors of MEA inside the tube are described in Figure 3. It is obvious that

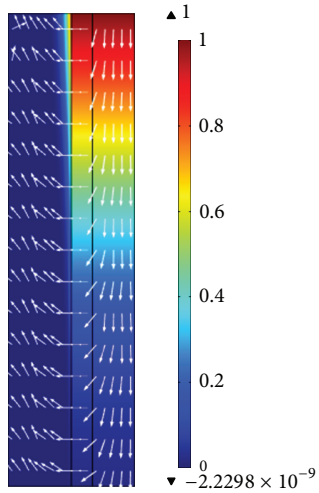

FIGURE 4: Flux vectors of CO_2 (C/C_0) in the model. $C_0 = 4\,\text{mol m}^{-3}$, $C_{MEA,0} = 12\,\text{mol m}^{-3}$, $v_{CO_2} = 0.2\,\text{m s}^{-1}$, and $v_{MEA} = 0.5\,\text{m s}^{-1}$.

the concentration of MEA gradually decreases from the inlet ($z = 0$) to the outlet ($z = L$). At the middle of the tube side, the concentration of MEA is higher than the other parts. But the minimum of the CO_2 concentration distribution and flux vectors is below $2\,\text{mol m}^{-3}$ at the tube-membrane interface because of the chemical reaction between CO_2 and MEA.

Figure 4 depicts the concentration gradient and the total flux vectors of CO_2 in the hollow fiber membrane model. The gas flows from the inlet of the shell side ($z = L$), while the absorbent flows in a countercurrent from the inlet of the tube side ($z = 0$). Initially, the concentration of CO_2 inside the fiber is assumed to be zero. Then CO_2diffuses and flows into the shell side through the membrane pores owing to the variation of the gas concentration.

Figure 5 shows the average CO_2 concentration inside the membrane contactor module in the radial direction. It can be seen from the diagram that the values in the membrane and shell side are roughly the same around $2.75\,\text{mol m}^{-3}$. However, as there are effects of the diffusion and chemical reaction in the tube, the value rapidly drops to zero in the center of the membrane contactor.

In order to find out the optimal conditions, the removal efficiency is the most significant measurable indicator concerning the whole absorption process. The equation for calculating the percentage of CO_2 removal is

$$w = \left[\frac{(vC)_{\text{inlet}} - (vC)_{\text{outlet}}}{(vC)_{\text{inlet}}}\right] \times 100\%, \tag{14}$$

where v is the volumetric flow rate and C is the average concentration of CO_2 inside the shell in the axial direction. Because the change of volumetric velocity in the shell side could be neglected and C_0 is the CO_2 concentration at the inlet of the shell, (14) can be estimated by

$$w = \left(1 - \frac{C_{\text{outlet}}}{C_0}\right) \times 100\%. \tag{15}$$

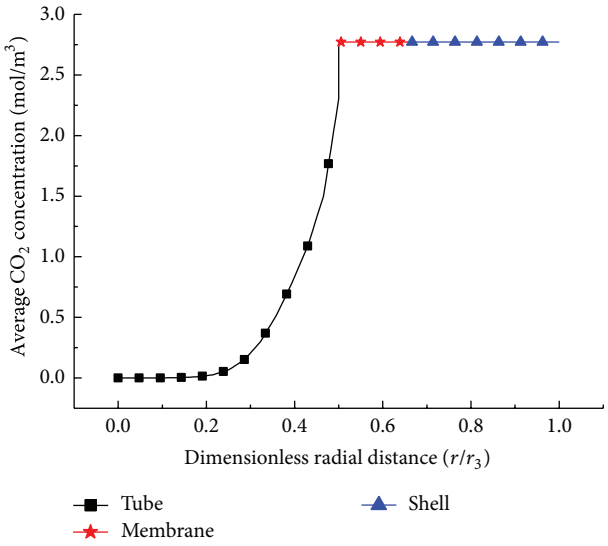

FIGURE 5: Concentration distribution of CO_2 in radial direction. $C_0 = 4\,\text{mol m}^{-3}$, $C_{MEA,0} = 12\,\text{mol m}^{-3}$, $v_{CO_2} = 0.2\,\text{m s}^{-1}$, $v_{MEA} = 0.5\,\text{m s}^{-1}$.

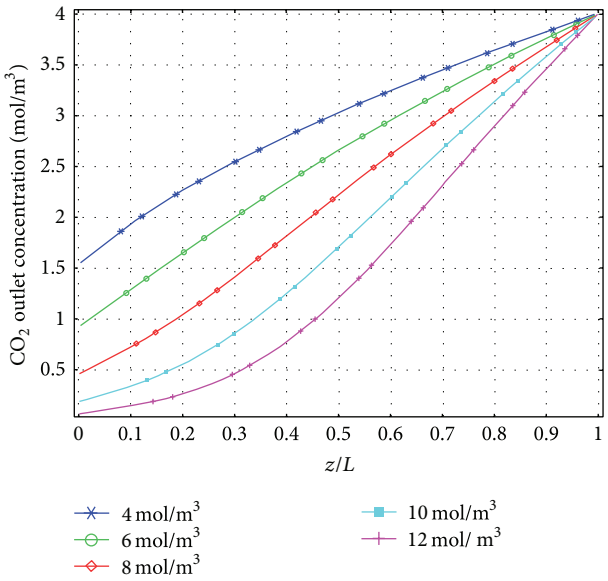

FIGURE 6: CO_2 concentration distribution along the membrane length. $C_0 = 4\,\text{mol m}^{-3}$, $v_{CO_2} = 0.2\,\text{m s}^{-1}$, $v_{MEA} = 0.5\,\text{m s}^{-1}$.

4.3. Effect of MEA Concentration. A set of MEA solutions with different concentrations including 4, 6, 8, 10, and $12\,\text{mol m}^{-3}$ are studied in this part. It can be clearly seen from Figure 6 that the outlet CO_2 concentration gradually declines with the gradual rise in MEA consistence. As using $4\,\text{mol m}^{-3}$ MEA the CO_2 concentration represents approximately $1.5\,\text{mol m}^{-3}$ CO_2, while the value is about $0.05\,\text{mol m}^{-3}$ using $12\,\text{mol m}^{-3}$ MEA solution. Meanwhile, Figure 2 shows an upward trend in the CO_2-removal percentage. Under the same conditions, it can be noticed that

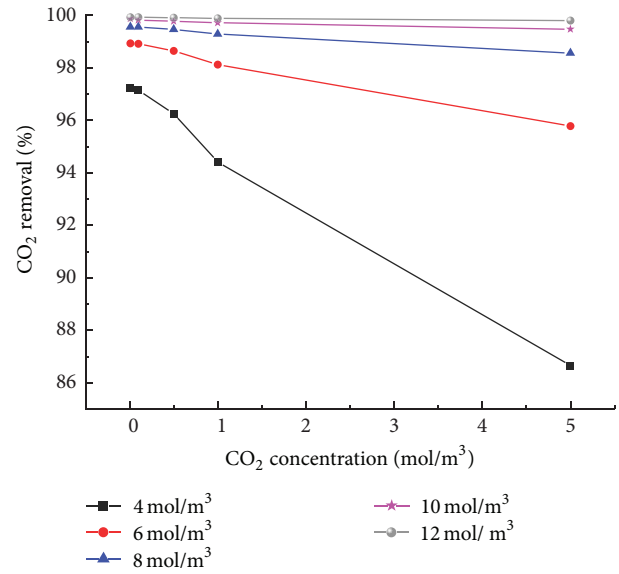

FIGURE 7: Removal percentage under different gas concentration. $r_1 = 0.15\,\text{mm}$, $r_2 = 0.2\,\text{mm}$, $r_3 = 0.3\,\text{mm}$, $L = 900\,\text{mm}$, $v_{CO_2} = 0.2\,\text{m s}^{-1}$, and $v_{MEA} = 0.5\,\text{m s}^{-1}$.

the percentage remains over 95 percent as the MEA concentration is higher than $10\,\text{mol m}^{-3}$. Hence, higher initial MEA concentration has higher removal percentage, which is beneficial to carbon capture.

4.4. Effect of CO_2 Concentration. The effect of different gas concentration on the CO_2-removal percent is described in Figure 7. With the augment in CO_2 concentration, the removal percentage of the absorption process slightly declines, but the minimum still remains around 87%. Particularly lower CO_2 concentration shows better absorption efficiency. So it can be seen from the graph that higher CO_2 percent has a negligible influence on the total percentage of CO_2 capture using MEA solution.

4.5. Effect of Gas Velocity. Figure 8 shows the percent CO_2 removal decreases by increasing the gas flow rates. It is noticed that lower gas velocity beneath $0.1\,\text{m s}^{-1}$ performs well whatever the MEA concentration is. However, higher gas flow rate has an adverse performance in removal of CO_2, because the residence time reduces in the membrane contactor. And the reaction and the dissolution between liquid and gas are insufficient inside this module, which cuts down the concentration gradient of CO_2 in the axial direction.

4.6. Effect of Absorbent Velocity. Figure 9 indicates the change of removal efficiency caused by a function of absorbent velocity. It is evident that the fraction of CO_2 removal goes up when increasing the solvent velocity. Meanwhile, it can be seen from the line chart that the liquid flow rate is a significant factor of absorption when the liquid concentration is comparatively low. The figure also reveals that the MEA

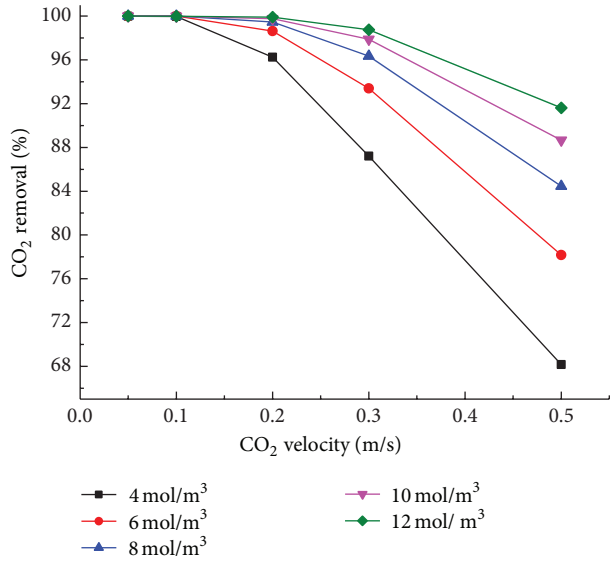

FIGURE 8: Removal percentage under different gas velocity. r_1 = 0.15 mm, r_2 = 0.2 mm, r_3 = 0.3 mm, L = 900 mm, C_0 = 0.5 mol m^{-3}, and v_{MEA} = 0.5 m s^{-1}.

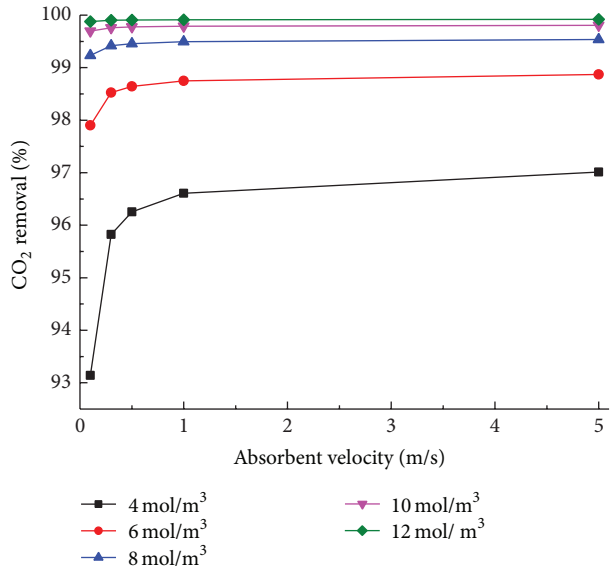

FIGURE 9: Removal percentage under different liquid velocity. r_1 = 0.15 mm, r_2 = 0.2 mm, r_3 = 0.3 mm, L = 900 mm, C_0 = 0.5 mol m^{-3}, and v_{CO_2} = 0.2 m s^{-1}.

velocity increases to above 1 m s^{-1}; however, the percent CO_2 removal shows no changes. That is, the absorption is less dependent on the absorbent velocity at higher flow rates.

5. Conclusions

This paper sets up a comprehensive 2D mathematical model for chemical absorption of pure CO_2 under nonwetting condition in a PP hollow membrane contactor. Meanwhile, the effect of the concentration and velocity of both liquid and gas and radial and axial diffusion in a HFMC model were considered in this work. In the case of using MEA aqueous solution, the modeling results and experimental data showed that the removal efficiency rose with an increase of the velocity and concentration of MEA, which was similar to others' work [21, 22]. However, as the liquid flow rate rose to 1 m s^{-1}, the percent of CO_2 removal was nearly constant. On the other hand, higher velocity and concentration of gas led to the opposite effect on absorption performance. Amongst them, the most proper parameters were less than 1 mol m^{-3} gas concentration and 0.2 m s^{-1} gas flow rate. Thus, these works are helpful for the selection of absorbents and gas compositions before experiments through comparing the removal rates. The following work will focus on the impacts of membrane properties and operating conditions on the absorption performance.

Nomenclature

K_{CO_2}: CO_2 total mass transfer coefficient (mol/(m^2 s kPa))
K_G: Total mass transfer coefficient (mol/(m^2 s kPa))
K_M: Membrane mass transfer coefficient (mol/(m^2 s kPa))
K_{N_2}: N_2 total mass transfer coefficient (mol/(m^2 s kPa))
K_g: Gas phase mass transfer coefficient (mol/(m^2 s kPa))
K_l: Liquid phase mass transfer coefficient (mol/(m^2 s kPa))
V_{in}, V_{out}: Gas phase volume flow rate (m^3/h).

Conflict of Interests

The authors declare that there is no conflict of interests regarding the publication of this paper.

Acknowledgments

This work was supported by the Fundamental Research Funds for the Central Universities (no. CDJZR12140034) and China National Tobacco Corp Chongqing Branch (no. NY20130501010010).

References

[1] Global CCS Institute, *The Global Status of CCS*, Global CCS Institute, Canberra, Australia, 2012.

[2] M. H. Al-Marzouqi, M. H. El-Naas, S. A. M. Marzouk, M. A. Al-Zarooni, N. Abdullatif, and R. Faiz, "Modeling of CO_2 absorption in membrane contactors," *Separation and Purification Technology*, vol. 59, no. 3, pp. 286–293, 2008.

[3] S. H. Lin, P. C. Chiang, C. F. Hsieh, M. H. Li, and K. L. Tung, "Absorption of carbon dioxide by the absorbent composed of piperazine and 2-amino-2-methyl-1-propanol in PVDF membrane contactor," *Journal of the Chinese Institute of Chemical Engineers*, vol. 39, no. 1, pp. 13–21, 2008.

[4] J. L. Li and B. H. Chen, "Review of CO_2 absorption using chemical solvents in hollow fiber membrane contactors," *Separation and Purification Technology*, vol. 41, no. 2, pp. 109–122, 2005.

[5] S. H. Yeon, K. S. Lee, B. Sea, Y. I. Park, and K. H. Lee, "Application of pilot-scale membrane contactor hybrid system for removal of carbon dioxide from flue gas," *Journal of Membrane Science*, vol. 257, no. 1-2, pp. 156–160, 2005.

[6] Z. Qi and E. L. Cussler, "Microporous hollow fibers for gas absorption. II. Mass transfer across the membrane," *Journal of Membrane Science*, vol. 23, no. 3, pp. 333–345, 1985.

[7] M. Al-Marzouqi, M. El-Naas, S. Marzouk, and N. Abdullatif, "Modeling of chemical absorption of CO_2 in membrane contactors," *Separation and Purification Technology*, vol. 62, no. 3, pp. 499–506, 2008.

[8] R. Faiz and M. Al-Marzouqi, "Mathematical modeling for the simultaneous absorption of CO_2 and H_2S using MEA in hollow fiber membrane contactors," *Journal of Membrane Science*, vol. 342, no. 1-2, pp. 269–278, 2009.

[9] M. Ghadiri, A. Marjani, and S. Shirazian, "Mathematical modeling and simulation of CO_2 stripping from monoethanolamine solution using nano porous membrane contactors," *International Journal of Greenhouse Gas Control*, vol. 13, pp. 1–8, 2013.

[10] H. Y. Zhang, R. Wang, D. T. Liang, and J. H. Tay, "Modeling and experimental study of CO_2 absorption in a hollow fiber membrane contactor," *Journal of Membrane Science*, vol. 279, no. 1-2, pp. 301–310, 2006.

[11] S. Eslami, S. M. Mousavi, S. Danesh, and H. Banazadeh, "Modeling and simulation of CO_2 removal from power plant flue gas by PG solution in a hollow fiber membrane contactor," *Advances in Engineering Software*, vol. 42, no. 8, pp. 612–620, 2011.

[12] S. Rajabzadeh, S. Yoshimoto, M. Teramoto, M. Al-Marzouqi, and H. Matsuyama, "CO_2 absorption by using PVDF hollow fiber membrane contactors with various membrane structures," *Separation and Purification Technology*, vol. 69, no. 2, pp. 210–220, 2009.

[13] S. Rajabzadeh, S. Yoshimoto, M. Teramoto, M. Al-Marzouqi, Y. Ohmukai, and T. Maruyama, "Effect of membrane structure on gas absorption performance and long-term stability of membrane contactors," *Separation and Purification Technology*, vol. 108, pp. 65–73, 2013.

[14] W. Rongwong, S. Assabumrungrat, and R. Jiraratananon, "Rate based modeling for CO_2 absorption using monoethanolamine solution in a hollow fiber membrane contactor," *Journal of Membrane Science*, vol. 429, pp. 396–408, 2013.

[15] J. G. Lu, A. C. Hua, Z. W. Xu, J. T. Li, S. Y. Liu, and Z. L. Wang, "CO_2 capture by membrane absorption coupling process: experiments and coupling process evaluation," *Journal of Membrane Science*, vol. 431, pp. 9–18, 2013.

[16] S. Boributh, R. Jiraratananon, and K. Li, "Analytical solutions for membrane wetting calculations based on log-normal and normal distribution functions for CO_2 absorption by a hollow fiber membrane contactor," *Journal of Membrane Science*, vol. 429, pp. 459–472, 2013.

[17] N. Ramachandran, A. Aboudheir, R. Idem, and P. Tontiwachwuthikul, "Kinetics of the absorption of CO_2 into mixed aqueous loaded solutions of monoethanolamine and methyldiethanolamine," *Industrial and Engineering Chemistry Research*, vol. 45, no. 8, pp. 2608–2616, 2006.

[18] D. Barth, C. Tondre, and J. Delpuech, "Stopped-flow investigation of the reaction kinetics of carbon dioxide with some primary and secondary alkanolamines in aqueous solutions," *International Journal of Chemical Kinetics*, vol. 18, no. 4, pp. 445–457, 1986.

[19] G. F. Versteeg, L. A. J. van Dijck, and W. P. M. van Swaaij, "On the kinetics between CO_2 and alkanolamines both in aqueous and non-aqueous solutions. An overview," *Chemical Engineering Communications*, vol. 144, no. 1, pp. 133–158, 1996.

[20] J. Happel, "Viscous flow relative to arrays of cylinders," *AIChE Journal*, vol. 5, no. 2, pp. 174–177, 1959.

[21] Z. F. Fan, G. C. Liu, Z. Wang, L. Yuan, and S. C. Wang, "Study on membrane gas absorption for CO_2 removal," *Membrane Science and Technology*, vol. 25, no. 5, pp. 34–39, 2005.

[22] S. Khaisri, D. deMontigny, P. Tontiwachwuthikul, and R. Jiraratananon, "CO_2 stripping from monoethanolamine using a membrane contactor," *Journal of Membrane Science*, vol. 376, no. 1-2, pp. 110–118, 2011.

[23] S. Paul, A. K. Ghoshal, and B. Mandal, "Removal of CO_2 by single and blended aqueous alkanolamine solvents in hollow-fiber membrane contactor: modeling and simulation," *Industrial and Engineering Chemistry Research*, vol. 46, no. 8, pp. 2576–2588, 2007.

[24] R. Faiz and M. Al-Marzouqi, "H_2S absorption via carbonate solution in membrane contactors: effect of species concentrations," *Journal of Membrane Science*, vol. 350, no. 1-2, pp. 200–210, 2010.